Sedimentation of Dilute and Semidilute Polymer Solutions at the Θ Temperature

Petar Vidakovic,† Catherine Allain,‡ and Francis Rondelez*

Physique de la Matière Condensée, Collège de France, 75231 Paris Cedex 05, France.
Received April 6, 1981

ABSTRACT: Sedimentation velocity techniques have been used to probe the dynamic properties of Θ polymer solutions. The measurements have been performed over a wide range of concentration and molecular weight for polystyrene in cyclohexane at 35.4 °C. Two distinct concentration regimes corresponding to dilute and semidilute (or entangled) solutions have been observed. They are delimited by a rather well-defined crossover concentration c^* which is much larger than for good solvents. The experimental results for the sedimentation coefficient are compared with the scaling law predictions. The agreement is excellent and allows measurement of the power-law dependences of the hydrodynamic radius R_H and dynamic correlation length ξ_H. R_H scales with molecular weight M as $M^{0.50\pm0.01}$, ξ_H scales with concentration as $c^{-0.96\pm0.04}$, and c^* scales with molecular weight as $M^{-0.50\pm0.01}$. The dilute regime has been extensively studied in the past and the observed exponents for R_H and c^* merely confirm well-known results. The determination of the exponent for ξ_H is more original and compares well with a very recent independent experiment by Roots and Nyström (*Macromolecules* **1980**, *13*, 1595).

I. Introduction

The statistics of flexible polymer chains are much easier to describe in Θ solvents than in good solvents. Indeed in that case, the attractive and repulsive interactions between monomers are exactly balanced out (at the Θ temperature) and the chains undergo ideal random flight statistics. The radius of gyration R_G takes a universal value independent of the exact chemical nature of the solvent and varies with molecular weight M as $M^{0.50}$.[1] Even the more refined theories that relate the Θ temperature to magnetic tricritical points have shown that deviations from ideality are logarithmically small and can be neglected in practice, at least in three-dimensional solutions.[2] Mean field calculations are therefore essentially correct although it is well-known that the recent approach based on scaling and renormalization group is theoretically more founded and encompasses both the good and Θ solvent cases.[3] The complete temperature–concentration diagram of polymer solutions has recently been deduced by Daoud and Jannink.[4] At the Θ temperature, they distinguish the dilute tricritical region, i.e., the so-called Θ region, and the semidilute and concentrated tricritical region, which had not been mentioned before. In all these domains, they have analyzed the behavior of the static correlations functions and derived the corresponding power-law exponents.

Experimentally, the situation is very surprising. There exist numerous data in dilute Θ solutions to measure the hydrodynamic radius R_H[5,6] and the coefficient k_s describing the concentration dependence of the hydrodynamic friction.[7] However, there are only few data at higher concentrations where the individual coils start to overlap (semidilute regime). To the best of our knowledge, when this work was started, there were only two published data of the static correlation length ξ_s, one by neutron scattering[8] and another by osmotic pressure experiments,[9] and several, nonsystematic measurements of its dynamic counterpart ξ_H by ultracentrifugation[9] and dynamic light scattering.[10] Such a scarcity of results can be explained from the fact that extremely high molecular weight materials have to be used in order to spread the semidilute regime over a large enough concentration range. This is a necessary condition to allow for a determination of the critical scaling power exponents with sufficient accuracy. Unfortunately, the rather compact ideal chain configuration raises the lower limiting concentration values and therefore compresses the span of the semidilute regime. Too high concentrations also cannot be used without breaking the scaling assumption that the friction between polymer and solvent dominates over the friction between monomers.[11] In that latter case the behavior is then much less universal.

This situation has prompted us to start an extensive study of the dynamic properties of polymer solutions at the Θ temperature by sedimentation velocity techniques. Polystyrene has been chosen since well-characterized high molecular weight fractions are easily available. The experiments have been performed over a wide range of concentrations, 10^{-4}–10^{-1} g/cm^3, and of molecular weights, 4×10^5–2×10^7. A brief report of our work has been given elsewhere.[12] We give here the full account of our results, which encompass both the dilute and the semidilute regimes. We are able to derive from our data the molecular weight dependence of the hydrodynamic radius of gyration R_H for isolated coils and of the crossover concentration c^* between the two concentration regimes. We also measure the concentration dependence of the density–density correlation length ξ_H in the semidilute regime. In section II, we briefly recall the theoretical predictions for the sedimentation coefficient in polymer solutions. In section III, we describe our experimental setup and materials. In section IV, we discuss our data analysis and show the necessity of correcting the data for the dilution and hydrostatic pressure effects that inevitably occur during centrifugation runs. The various results are presented in section V and compared with the existing literature data in section VI. In the Conclusion, we emphasize that the dynamic critical exponents for the various physical observables in Θ polymer solutions are in good agreement with the theoretical predictions.

II. Theoretical Background

It is well-known that the sedimentation coefficient s can be directly related to the mass of the sedimenting object M and to its friction factor f by the formula[13]

$$s \propto M/f \tag{1}$$

where $f = 6\pi\eta R_H$ and R_H is the hydrodynamic radius of gyration. Therefore, the molecular dependence of the

† On leave of absence from Prirodno-matematicki fatkultet Odsek za fizicke i meteoroloske nauke, Studentski trg 16 P.B. 550, Belgrade, Yougoslavie.

‡ Permanent address: Laboratoire de Spectroscopie Hertzienne, Ecole Normale Supérieure, rue Lhomond, 75005 Paris, France.

0024-9297/82/2215-1571$01.25/0 © 1982 American Chemical Society

hydrodynamic radius of gyration can be easily extracted from sedimentation data in dilute solutions. If s scales as M^{β}, R_H scales as $M^{1-\beta}$.

The situation is obviously more complex in semidilute solutions, where the chains are entangled. In 1977, Brochard and de Gennes[14] proposed a simple scaling law for s, independent of the molecular weight

$$s \sim c^{-\alpha} \tag{2}$$

where c is the polymer concentration and α a characteristic scaling exponent.

Starting from a Kubo formula involving static correlation functions, they have been able to reduce their results to a clear qualitative picture: an entangled polymer chain behaves like a sequence of N/g blobs, each occupying a volume ξ_s^3 and having the same number of monomers $g = c\xi_s^3$. Since ξ_s is the pair correlation distance but also the correlation length for hydrodynamic interactions, these blobs can be considered as independent moving units. Taking a Stokes friction factor $6\pi\eta\xi_H$ for one blob and using the two-fluid model introduced by de Gennes,[11] they obtained a Darcy law for the permeation of solvent through a porous plug of polymer solution. The corresponding permeability coefficient λ can be written[14]

$$\lambda = g/6\pi c\xi_H \tag{3}$$

According to ref 4, the static correlation function should scale as $\xi_s \propto c^{-1}$ in Θ solvents. Following the scaling approach, it is reasonable to assume that the same form can be taken in experiments which measure dynamic correlations; i.e., $\xi_H \propto \xi_s$.[15] Therefore, $\lambda \sim c^{-2}$ in Θ solvents. Minjlieff and Jaspers[16] have shown that there exists a straightforward relation between the sedimentation and the permeability coefficients

$$s \propto \lambda c \tag{4}$$

Therefore, the final result is

$$s \sim c^{-1} \tag{5}$$

The same concentration dependence can be derived even more directly by replacing the total mass of the chain in the equation for dilute solutions by the mass of one blob M_b and similarly the total friction factor by the blob friction factor $f_b \propto \eta\xi_H$

$$s \propto M_b/\eta\xi_H$$

Since $g = c\xi_s^3$, we get

$$s \propto \frac{g}{\eta\xi_H} \propto \frac{c\xi^2}{\eta} \sim c^{-1} \tag{6}$$

Thus the sedimentation coefficient of polymers in semidilute solutions is predicted to be power-law dependent on concentration but independent of molecular weight.

The crossover between the dilute and semidilute concentration regimes occurs for a concentration c^* which corresponds to the onset of overlap between chains. c^* is obtained when the average local monomer density inside a single chain is equal to the macroscopic monomer concentration: $c^* \propto M/R_G^3$. There is, however, an unknown proportionality factor, which can only be determined experimentally.

III. Experimental Section

Materials and Sample Preparation. Narrow molecular weight fractions of polystyrene were obtained from Toyo Soda Co., Ltd., Japan and used as received. Other fractions from Pressure Chemical Co. were also used in some cases but were generally found to be of inferior quality. Their specifications are listed in Table I.

Table I
Manufacturers' Specifications for the Polystyrene Fractions

grade	lot no.	nominal mol wt	M_w/M_n
F-2000	TS-33	2060×10^4	not defined
F-850	TS-31	842×10^4	1.17
F-380	TS-34	384×10^4	1.05
F-126	TS-8	126×10^4	1.05
P-600	PC-60914	600000	≤ 1.1
F-40	TS-6	42.2×10^4	1.04

The preparation of well-dispersed solutions in cyclohexane was a crucial experimental point. Early direct dissolution attempts into hot cyclohexane (45 °C) were found to give irreproducible results, especially with the high molecular weight fractions. This problem was overcome by a two-step procedure. The chains were first dissolved in spectroscopic grade benzene (Merck) at extremely low concentrations ($<10^{-4}$ g/cm^3) and were lyophilized overnight. The fluffy powder obtained was then added grain by grain into hot spectroscopic grade cyclohexane. Solutions were prepared by weighing. Great care was taken to prevent shear degradation of the polymer solutes. No mechanical stirring was ever applied to the solutions, which were kept at 45 °C until just before use. The solutions were then injected with a syringe in the sedimentation cell, except for three concentrations of the 8.42×10^6 polymer (2.2×10^{-2}, 5.1×10^{-2} and 8×10^{-2} g/cm^3) that were too viscous and had to be prepared directly in the cell.

Sedimentation Experiments. A Spinco Model E analytical ultracentrifuge was used in conjunction with a Schlieren optical system. The cell was a 4° single sector, 12 mm thick × 15 mm long. The displacement of the sedimentation boundary with time was recorded on a photographic plate and later analyzed with a profile projector. Fourteen successive pictures were generally taken during which the solvent–solution boundary was allowed to move over the longest possible distance within the cell ($\simeq$10 mm) to improve the measuring accuracy. Precision of the readings was always better than 1%. Most sedimentation runs were performed at a rotor speed of 30 000 rpm but different speeds, between 15 000 and 52 000 rpm, were sometimes used to check the influence of the hydrostatic pressures generated within the cell. The temperature was controlled to ±0.1 °C by a RTIC unit. The rotor was preheated to 40 °C externally and slowly brought to its final temperature after positioning of the sample cell. The Θ temperature of the polystyrene–cyclohexane solutions was taken to be 35.4 °C, as determined by Slagowski et al.[17] It was also checked that temperature variations as large as 1 °C around the Θ temperature did not affect the results, at least in the concentration range studied here ($c > 10^{-4}$ g/cm^3). This has been confirmed recently by Swislow et al.[18] in the course of their study on chain collapse below the Θ temperature. The temperature dependence of the hydrodynamic radius of gyration R_H and correlation length ξ_H has been analyzed quantitatively by Adam and Delsanti.[10] They get $R_H \sim (T - \Theta)^{0.034\pm0.005}$ and $\xi_H \sim (T - \Theta)^{-0.33\pm0.04}$ in the vicinity of the Θ temperature.

IV. Data Analysis

By definition, the sedimentation coefficient s is written as

$$s = \frac{1}{\omega^2}\frac{d}{dt}\ln r_H \tag{7}$$

where ω is the angular rotor speed and r_H the distance of the sedimentation peak from the rotation axis, as measured with the Schlieren optics.[13] s is generally derived by plotting $\ln r_H$ vs. the elapsed time t during the centrifugation run. In the most simple cases, the variation is linear and s is directly obtained from the average slope. However, two spurious effects come into play to complicate that picture. The first is the radial dilution due to the sector shape of the sample cell. The second is the hydrostatic pressure exerted by the liquid column between the solvent–air meniscus and the pure solvent–solution boundary.

These effects have been amply recognized in the past and are well described in the book of Fujita.[19] Nevertheless, in polymer solutions, the concentration dependence of the sedimentation coefficient is not as simple as in ordinary solutions. For instance in section II, we have shown that in the semidilute regime, s varies like c^{-1}. Therefore, even the detailed studies of Dishon,[20] valid for dilute polymer solutions where s varies like $(1 + k_s c)^{-1}$, cannot be applied in that case. We present here a general description for all kinds of concentration and pressure dependences, but we neglect the diffusion processes responsible for the broadening of the sedimentation peak.

(a) Radial Dilution. If we call c_p the polymer concentration in the plateau region and c_m the initial filling concentration, we can write

$$c_p/c_m = [r_m/r_H]^2 \tag{8}$$

Typically for $r_m = 6$ cm, a displacement of the solution boundary over 1 cm leads to a 20% dilution effect on concentration because of the sector shape of the cell. We will now show that this radial dilution introduces a curvature in the ln r_H vs. t curves. Indeed, since s is concentration dependent, the measured value s_{app} will be a function of the peak boundary position. The true sedimentation coefficient s will only be obtained by extrapolating the measurement to the meniscus position where the solution concentration is identical with the initial filling concentration c_m.

In the most general case, the concentration dependence of s can be described as

$$s_{app}(r_H) = s\frac{f(c_p)}{f(c_m)} = \frac{1}{\omega^2}\frac{d}{dt}\ln\frac{r_H}{r_m} \tag{9}$$

As the displacements are small ($r_H/r_m \simeq 1$), we can develop to first order in a Taylor expansion. After integration, we get

$$\frac{1}{\omega^2 t}\ln\left(\frac{r_H}{r_m}\right) = s\left(1 - c_m s\omega^2 t\frac{f'(c_m)}{f(c_m)}\right) \tag{10}$$

The dilution effect transforms the linear dependence of ln (r_H/r_m) vs. time t into a quadratic one, at least to the first order:

$$\ln (r_H/r_m) = s\omega^2 t + A_{rd}t^2 \tag{11}$$

with

$$A_{rd} = -c_m s^2\omega^4 f'(c_m)/f(c_m) \tag{12}$$

We can now specify more explicity the analytical form of f. In the dilute regime, an often-used expression is $f = (1 + k_s c)^{-1}$, where k_s is the concentration coefficient related to the hydrodynamically effective volume per gram of solute and is characteristic of the polymer–solvent pair.[21] Therefore

$$A_{rd} = c_m s^2\omega^4 k_s(1 + k_s c_m)^{-1} \tag{13}$$

For a polystyrene chain of $M = 10^6$ in cyclohexane, $k_s \simeq 4.5 \times 10^{-4}M^{1/2} = 0.45$ cm^3/g and $s = 1.5 \times 10^{-15}M^{1/2} = 15$ S (1 S = 10^{-13} s).[5] Taking $c_m = 10^{-4}$ g/cm^3 and $\omega = 30\,000$ rpm = 3140 s^{-1}, one gets $A_{rd} \simeq 10^{-14}$ s^{-2}.

In the semidilute regime, it is predicted that $s \sim c^{-1}$ (see section II). Therefore, $f'(c_m)/f(c_m) = -c_m^{-1}$ and A_{rd} takes the simple form

$$A_{rd} = s^2\omega^4 \tag{14}$$

independent of concentration. For $\omega = 30\,000$ rpm and a typical value of $s = 5$ S in the semidilute concentration range, one gets $A_{rd} \simeq 2.5\ 10^{-11}$ s^{-2}.

It is important to note that several features are common to the dilute and semidilute regimes. In both cases A_{rd} varies with the square of the true sedimentation coefficient s and with the fourth power of the rotor speed ω and takes also relatively small values. Moreover, A_{rd} is always positive, which means that the apparent sedimentation coefficient is increased. Due to the dilution effect, the plot of ln r_H vs. time will exhibit an upward curvature. An example of such behavior is given in Figure 2.

(b) Hydrostatic Pressure. The liquid column of pure solvent between the meniscus and the solution boundary exerts very large hydrostatic pressures P on the polymer solution, especially at high centrifugal speeds.

$$P = \tfrac{1}{2}\rho_0^0\omega^2(r_H^2 - r_m^2) \tag{15}$$

ρ_0^0 is the solvent density at atmospheric pressure. Typically, for $r_m = 6$ cm, the pressure exerted at the bottom of the cell, i.e., $r_H = 7.2$ cm is $P = 60$ atm for $\omega = 30\,000$ rpm. This monotonic pressure increase progressively changes the physical parameters of the polymer solutions, e.g., friction coefficient and partial specific volume of the solute, density of the solution, etc.[5] The sign of the effect on the apparent sedimentation coefficient is not trivial. For polymer solutions, it is experimentally observed that the apparent sedimentation coefficient decreases when pressure is increased.[5,22,23] Quantitatively, we can use the same approach as for radial dilution and write

$$s_{app}(r_H) = sf(P)|_{r=r_H} \tag{16}$$

where $f(P)$ is an analytical function such that $f(P) = f(P_0) = 1$ for $r = r_m$. Therefore, the sedimentation equation can be developed to first order as

$$\frac{1}{\omega^2 t}\ln\frac{r_H}{r_m} = s\left(1 + \frac{1}{2}\rho_0^0 s\omega^2 r_m^2 t\frac{f'(P_0)}{f(P_0)}\right) \tag{17}$$

s is the true value of the sedimentation coefficient as measured on the meniscus position r_m, i.e., at atmospheric pressure P_0.

The pressure effect introduces a quadratic dependence of ln (r_H/r_m) as a function of the elapsed time t:

$$\ln (r_H/r_m) = s\omega^2 t + A_{press}t^2 \tag{18}$$

with

$$A_{press} = \frac{1}{2}\rho_0^0 s^2\omega^6 r_m^2\frac{f'(P_0)}{f(P_0)} \tag{19}$$

Empirically, the form $f(P) = 1 - \mu P$ is generally adopted, where μ is a pressure coefficient characteristic of the polymer–solvent system. Therefore

$$A_{press} = -\tfrac{1}{2}\rho_0^0 s^2\omega^6 r_m^2\mu \tag{20}$$

Since μ is positive, this relationship implies a negative value for A_{press}. Because of the pressure effect, the plot of ln r_H vs. time will exhibit a downward curvature, contrary to the dilution effect. Another difference is that A_{press} depends on the sixth power of the rotor speed, instead of the fourth power. This will allow for a separation of the two effects simply by performing a set of experiments at various rotor speeds but at fixed concentration. Taking $\mu \simeq 10^{-8}$ Pa^{-1},[5,23] typical values of A_{press} can be calculated in the two limiting cases where s is either large or small. If $s = 60$ S, $A_{press} \simeq -10^{-9}$ s^{-2} whereas $A_{press} \simeq -3 \times 10^{-13}$ s^{-2} if $s = 1$ S. It is clear that the importance of the pressure effect is critically dependent on the actual value of the sedimentation coefficient.

(c) Radial Dilution Combined with Hydrostatic Pressure. During a centrifugation run, the two effects

of radial dilution and hydrostatic pressure are present simultaneously. Dishon[20] has performed the exact calculation for dilute polymer solutions. However, it will be sufficient for our needs to consider these two effects as uncoupled in first approximation and to simply add them.

$$\ln (r_H/r_m) = s\omega^2 t + A_{total}t^2 \quad (21)$$

with

$$A_{total} = -c_m s^2\omega^4 \frac{f'(c_m)}{f(c_m)} + \frac{1}{2}\rho_0{}^0 s^2\omega^6 r_m{}^2 \frac{f'(P_0)}{f(P_0)} \quad (22)$$

In the case of ordinary solutions (where $f(c) = (1 + k_s c)^{-1}$ and $f(P) = 1 - \mu P$), we can compare our expression to eq 30 of ref 20. The results are identical in the limit of validity of our calculation, i.e., to first order in k_s and μ.

With regard to the contribution of the diffusion process we can show that it is negligible in our experiments.

In the dilute regime, the self-diffusion coefficient of one chain is of the order of 2×10^{-7} cm^2/s for a polystyrene chain of $M \simeq 10^6$. In the semidilute regime, the cooperative diffusion coefficient is also of the same order of magnitude. Using the Einstein law to calculate the diffusion broadening Δr_H of the sedimentation peak, we obtain $\Delta r_H = (2Dt)^{1/2} \simeq 400$ μm during a typical sedimentation time $t = 1$ h. This is negligible compared to the total peak displacement ~ 1 cm, as directly observed on the schlieren pictures. Detailed calculations by Dishon[20] show that the error introduced by neglecting diffusion is $\sim 2\%$ on the various parameters.

In the following, we will always perform a best fit of the experimental data point with a quadratic function of time. Earlier workers[22] have sometimes adopted a simpler procedure in which they perform their various sedimentation runs at the same rotor speed and over the same sedimentation distance. Consequently, they believe that their data are simply shifted always by the same correction factor. However, this is clearly incorrect since the quadratic coefficient A_{total} depends on the initial concentration c_m, either directly or by the s^2 term. Its importance relative to the linear coefficient $s\omega^2$ will therefore be different for experiments performed at different concentrations.

We have used two different criteria to evaluate the quality of our fitting procedures. First, we calculate the well-known χ^2 test

$$\chi^2 = \sum_i \epsilon_i{}^2 / \sum_i \psi_i{}^2 \quad (23)$$

where

$$\epsilon_i = (\ln r_H)_{exptl} - (\ln r_H)_{calcd}$$

and

$$\psi_i = (\ln r_H)_{exptl}$$

Second, we calculate the Q factor introduced by Tournarie[24]

$$Q = 1 - \sum_i \epsilon_i\epsilon_{i+1} / \sum_i \epsilon_i{}^2 \quad (24)$$

The higher the Q value, the better the fit. For $Q < 0.8$, it can be considered that the fitting function is not adapted to the experimental points and that there are systematic deviations with the calculated points.

V. Results

Figure 1 displays a typical sedimentation velocity plot showing ln r_H vs. time, where r_H is the position of the pure solvent–solution boundary. In this particular example the solute molecular weight was 3.84×10^6, the initial filling concentration was $c = 1.92 \times 10^{-2}$ g cm^{-3}, and the rotor speed was $\omega = 40\,000$ rpm, i.e., fairly high. It is noticeable on the figure that the data points exhibit a slight but definite downward curvature. This is best demonstrated by fitting the experimental points successively to a linear (Figure 1, top) and to a quadratic (Figure 1, bottom) polynomial. It is only in the latter case that the differences (represented by the crosses) between experimental and calculated points are randomly distributed around the null value. More quantitatively, the χ^2 factor of fit goodness changes from 3.5×10^{-6} to a very good 3.6×10^{-8}. Similarly, the Q factor changes from 0.32 to a very good 1.51.

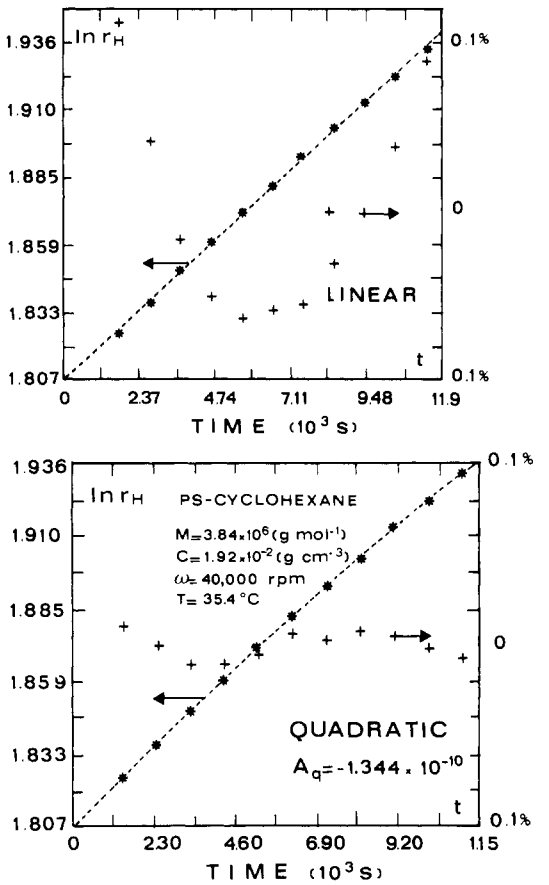

Figure 1. Sedimentation peak boundary position r_H vs. elapsed time t. The same experimental data points (*) have been reported twice on semilog scales. They have been adjusted to linear and quadratic functions (dotted lines) in the upper and lower pictures, respectively. In each case, the relative deviations (+) between experimental and calculated points have also been plotted. Note the much better agreement with quadratic functions $A_q t^2 + B_q t$. A_q is negative in the present experimental conditions. $A_q = -1.34 \times 10^{-10}$ s^{-2} and $s_q = B_q/\omega^2 = 7.37 \times 10^{-13}$ s^{-1}.

Figure 2 shows another set of data points obtained under conditions close to those of Figure 1, $c = 0.8 \times 10^{-2}$ g cm^{-3} and $M = 8.4 \times 10^6$, but for a lower rotor speed, $\omega = 29\,819$ rpm. Again the fit to a quadratic polynomial is much better, as clearly observed when the linear and quadratic plots of Figure 2 are compared. The curvature of the experimental points is upward, as opposed to the previous case.

It is therefore clear that the quadratic coefficient A_q of the $\ln (r_H/r_m) = A_q t^2 + B_q t + C$ equation is a sensitive function of rotor speed and can adopt both positive and negative values.

We have performed systematic measurements of A_q as a function of the three essential experimental parameters: rotor speed, concentration, and molecular weight. The results obtained at a single concentration but variable

Table II
Values of A_q and B_q for the 20.6×10^6 Polystyrene Fractions at $c = 3.7 \times 10^{-4}$ g cm^{-3} [a]

run no.	ω, s^{-1}	A_q	B_q	$10^{13}s_q$, s	Q_q	error on A_q (program)	$10^{13}s_{lin}$, s	Q_{lin}	r_m, cm	no. of points
1	2094.4 (20000 rpm)	-5×10^{-11}	2.8×10^{-5}	64.62	1.14	1×10^{-11}	63.82	0.67	5.942	42
2	2729.4 (26064 rpm)	-4.3×10^{-10}	4.7×10^{-5}	63.62	1.01	9×10^{-11}	61.33	0.33	5.912	30
3	3141.6 (30000 rpm)	-9.3×10^{-10}	6.3×10^{-5}	64.24	0.83	5×10^{-10}	61.82	0.54	6.027	18
4	3576.2 (34150 rpm)	-2.3×10^{-9}	8.2×10^{-5}	65.18	0.92	6×10^{-10}	60.42	0.39	5.930	19
5	4225.4 (40350 rpm)	-5.3×10^{-9}	1.1×10^{-9}	65.35	0.77	9×10^{-10}	58.54	0.54	5.950	10
6	5039.3 (48122 rpm)	-1.6×10^{-8}	1.5×10^{-4}	66.23	1.08	3×10^{-9}	56.40	0.65	5.942	9

[a] $s_q = B_q/\omega^2$, Q_q is the fit quality factor, and r_m is the meniscus position away from the rotor axis. s_{lin} and Q_{lin} stand for a fit to a linear function of time instead of quadratic.

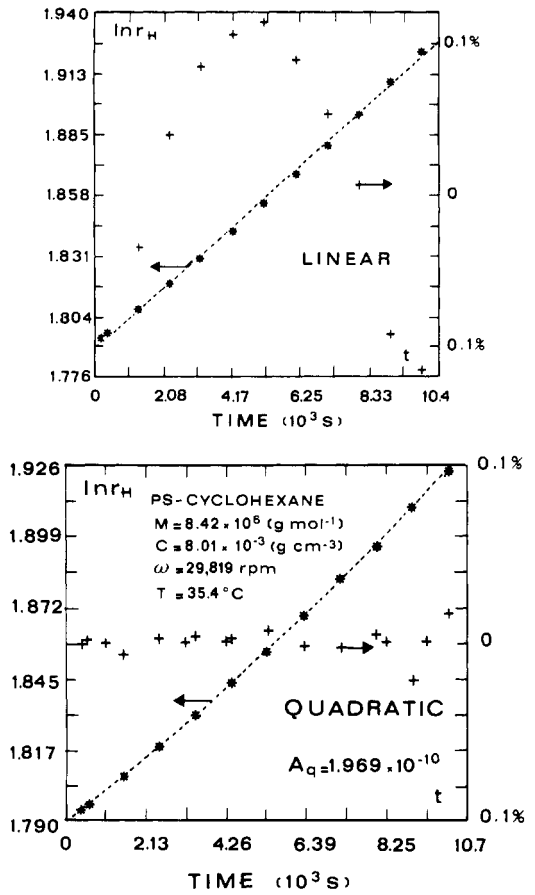

Figure 2. Sedimentation peak boundary position r_H vs. elapsed time t. The same experimental data points (*) have been reported twice on semilog scales. They have been adjusted to linear and quadratic functions (dotted lines) in the upper and lower pictures, respectively. In each case, the relative deviations (+) between experimental and calculated points have also been plotted. Note the much better agreement with quadratic functions $A_q t^2 + B_q t$. A_q is positive. $A_q = 1.97 \times 10^{-10}$ s^{-2} and $s_q = B_q/\omega^2 = 11.4 \times 10^{-13}$ s^{-1}.

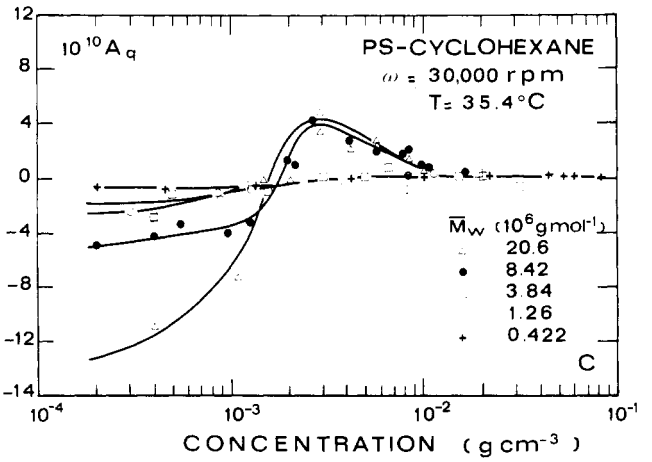

Figure 3. Dependence of the quadratic parameter A_q with polymer concentration for different molecular weight fractions. All measurements have been performed at the same rotor speed $\omega = 30\,000$ rpm.

speed on solutions of 20.6×10^6 molecular weight samples are collected in Table II. The values of the quality factor Q_{lin} and of the sedimentation coefficient s_{lin} in the case of a fit to a linear function of time are also indicated for comparison. The A_q values are all negative and change by more than 2 orders of magnitude when the rotor speed is increased by a factor of 2.5.

The statistical error on the fit determination of A_q is quite large and by no means negligible compared to the quoted A_q values. This is due to the small number of measurements during a sedimentation run (14 pictures are typical). It may thus seem surprising to insist on the necessity of fitting the data to quadratic polynomials. To prove this point, we have performed a numeric simulation by superposing a 5% statistical noise over the exact sedimentation peak positions calculated from eq 22 and using predetermined values for s_q and A_q, namely, $s = 10$ S and $A_q = -10^{-10}$ s^{-2}. A fit to a quadratic polynomial yields a sedimentation coefficient $s_q = 9.85$ S, i.e., within 2% of the true value, while A_q is found to be $-(9 \pm 1.5) \times 10^{-11}$ s^{-2}, i.e., within 10% only of the true value and with a 15% statistical error. On the other hand, a fit to a linear function of time yields $s_{lin} = 8.45$, i.e., 15% too low compared to the true value. Moreover, the quality factor of the fit drops to a low 0.44 value instead of 1.41 in the previous case. It can thus be concluded that the fitting of the data to a quadratic polynomial gives much more accurate sedimentation coefficient values even though the determination of the A_q coefficient is not very precise.

Next we have investigated, at fixed rotor speed, how A_q varies with sample molecular weight and concentration. This is done in Figure 3, in which A_q has been plotted vs. polymer concentration between 10^{-4} and 10^{-1} g cm^{-3} for five different molecular weight between 0.4×10^6 and 20.6×10^6. Three distinct regions are observed. Up to 10^{-3} g cm^{-3}, A_q is negative for all molecular weights, can take large absolute values, and is little dependent on the actual concentration. Above 10^{-2} g cm^{-3}, A_q is close to zero for all concentrations and molecular weights. In the intermediate regime, between 10^{-3} and 10^{-2} g cm^{-3}, it is more

Table III
Parameters of the Fit to Linear (lin) and Quadratic (q) Functions of Time for the 8.42×10^6 Polystyrene Fractions

10^4c, g cm^{-3}	$10^{13}s_{lin}$, s	10^5A_{lin}	Q_{lin}	$10^8X_{lin}^2$	$10^{13}s_q$, s	$10^{11}A_q$	Q_q	$10^8X_q^2$
1.98	39.63	3.85	1.14	3.16	39.97	−9.65	1.13	2.90
2.40	40.95	4.04	1.04	2.70	40.94	0.39	1.04	2.99
4.02	38.00	3.75	0.45	8.5	39.51	−42.1	0.84	0.74
5.46	39.93	3.93	0.65	10.7	41.19	−33.7	1.06	2.94
9.77	39.92	3.92	0.396	26.2	41.75	−40.7	1.00	2.13
12.2	39.36	3.88	0.46	13.9	40.72	−32.3	1.16	0.90
19.5	31.37	3.10	0.32	18.9	30.57	12.8	0.60	7.15
21.4	30.08	2.94	0.46	5.5	29.58	9.06	0.51	3.08
26.5	27.07	2.67	0.64	6.6	25.78	43.03	0.88	2.94
41.9	21.82	2.15	0.23	126.9	19.77	26.8	0.60	5.70
56.8	16.49	1.62	0.33	77.2	14.70	20.8	1.50	1.78
80.1	13.46	1.31	0.32	351.5	11.40	19.7	1.51	3.60
83.3	9.65	0.95	1.19	1.40	9.52	1.89	1.31	1.30
98.6	8.11	0.8	0.89	3.30	7.69	8.45	1.27	2.21
103	11.44	1.13	0.72	210.8	10.50	6.58	1.53	108.8
162	5.82	0.58	0.37	15.5	5.23	5.20	0.81	1.00
220	3.87	0.08	0.47	168	4.15	4.21	0.71	1.41
510	1.85	0.02	0.36	29.7	1.94	0.65	1.06	1.60
802	1.32	1.31	0.23	25.8	1.39	0.71	0.75	1.87

Table IV
Parameters of the Fit to Linear (lin) and Quadratic (q) Functions of Time for the 4.22×10^5 Polystyrene Fractions

10^4c, g cm^{-3}	$10^{13}s_{lin}$, s	10^6A_{lin}	Q_{lin}	$10^8X_{lin}^2$	$10^{13}s_q$, s	$10^{12}A_q$	Q_q	$10^8X_q^2$
2.00	9.05	8.88	0.60	30.1	9.66	−65.75	1.09	8.09
4.54	9.93	9.75	0.75	75.5	10.86	−95.74	1.47	29.7
42.1	8.94	8.77	0.82	6.1	9.09	−15.46	0.76	5.44
90.7	7.37	7.22	1.58	4.6	7.37	−0.12	1.58	4.91
212	5.10	5.00	0.50	5.4	4.92	8.76	0.84	2.17
249	3.68	3.60	0.64	31.8	3.48	5.98	0.99	4.43
302	3.80	3.72	1.28	49.2	3.79	8.56	1.13	4.49
451	2.51	2.47	0.55	27.7	2.39	2.35	0.89	6.91
532	1.76	1.73	0.53	61.3	1.81	−0.70	0.68	55.3
608	1.84	1.81	1.10	10.5	1.79	0.94	1.17	7.99
835	1.29	1.26	0.54	41.8	1.17	1.86	1.49	10.9

difficult to distinguish definite trends. It can only be said that A_q is mostly positive and seems to take larger values as the molecular weight is increased.

Once it has been realized that the experimental sedimentation curves have to be fitted with quadratic functions of time, the true value of the sedimentation coefficient s is readily extracted from the coefficient B_q of the quadratic polynomial $B_q = s\omega^2$. The complete results have been reported in Tables III and IV for two different molecular weights of 8.42×10^6 and 0.42×10^6 over 2 decades of concentration. The subscripts lin and q stand for the fits to linear and quadratic polynomials, respectively. The s_{lin} values are only given to show that fits to linear functions yield erroneous sedimentation coefficient values by as much as 20% in some cases. They will not be used in the remaining text.

The s_q values have been plotted as a function of polymer concentration in Figure 4 for all molecular weights. Logarithmic scales have been used for both coordinates. The curves display the characteristic tree-like appearance already observed for polymer in good solvents.[25] At high concentrations, all the data points collapse onto a master curve, irrespective of chain molecular weight. This common branch is steeply decreasing with polymer concentration. On the contrary, in the low concentration range, the s data are markedly dependent on molecular weight but show little variation with the actual solution concentration. The transition between these two regimes of concentration occurs for a rather sharply defined value c^*, which is itself molecular weight dependent. Its estimation for each molecular weight fraction is indicated by the arrows in Figure 4, which show the intersection between the master curve at high concentration and the nearly horizontal curves passing through the data points at low concentrations.

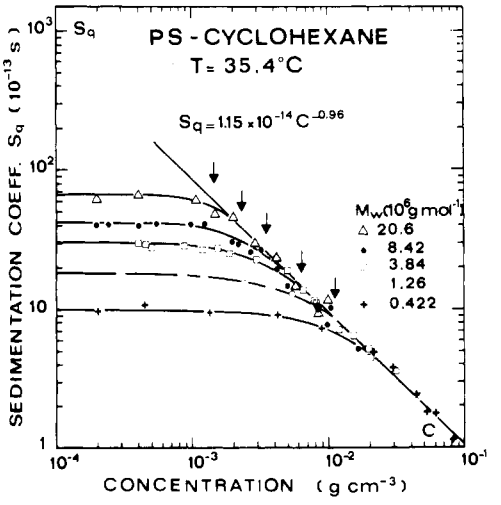

Figure 4. Sedimentation coefficient s_q of polystyrene in cyclohexane vs. polymer concentration c for five different molecular weight fractions. s_q is derived from the best fit to a quadratic function for ln r_H vs. t (see text). The solid line represents a power-law dependence $s_q \propto c^{-\alpha}$, with $\alpha = 0.96$ in the high-concentration, semidilute range. The arrows indicate the concentrations of crossover to the semidilute regime for the different fractions.

It is possible to derive from the results of Figure 4 several power laws vs. molecular weight and concentration. This is done in Figures 4–6.

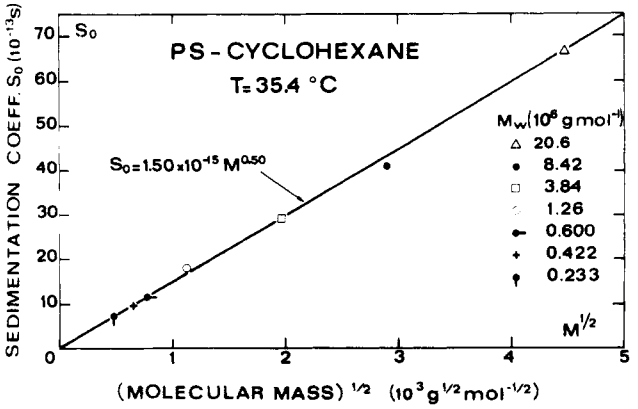

Figure 5. Sedimentation coefficient of polystyrene chains at infinite dilution s_0 vs. square root of molecular mass $M^{1/2}$. The data points fall on a straight line $s_0 = 1.50 \times 10^{-15} M^{0.50}$. The point corresponding to 233 000 molecular weight has been taken from ref 21.

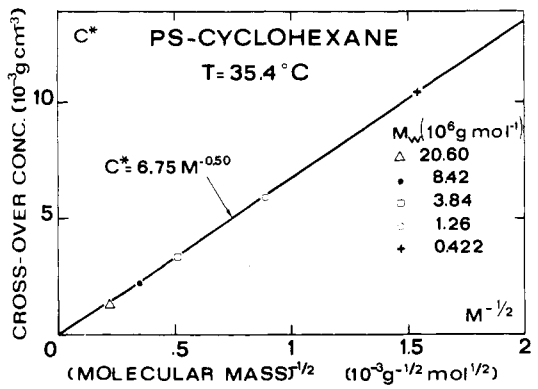

Figure 6. Crossover concentration c^* between the dilute and semidilute regimes, as deduced from Figure 4, vs. inverse root square of molecular weight $M^{-1/2}$. The data points fall on a straight line $c^* = 6.75 M^{-0.50}$.

Table V
Sedimentation Values at Infinite Dilution

$10^{-6} M_w$	$10^{13} s_0$, s	$10^{-6} M_w$	$10^{13} s_0$, s
20.6	66.7	0.600	11.6
8.42	40.8	0.422	9.7
3.84	29.4	0.233	7.3
1.26	18.2		

In the high-concentration regime, a least-squares fit combining 26 data points that are found to be independent of molecular weight gives a straight line of slope −0.96 ± 0.04 (Figure 4). Therefore

$$s_q = 1.15 \times 10^{-14} c^{-0.96}$$

In the low-concentration regime, the s_q values for the various fractions can be extrapolated to infinite dilution by making a plot of s_q^{-1} vs. concentration. The results are given in Table V. The molecular weight of $s_q(c \to 0) = s_0$ is observed to be (Figure 5)

$$s_0 = (1.50 \pm 0.01) \times 10^{-15} M^{0.50} \text{ S}$$

in the present experimental range of (0.23–20.6) × 10^6.

Last, the crossover concentration c^* decreases with molecular weight (Figure 6) as

$$c^* = (6.75 \pm 0.09) M^{-0.50}$$

VI. Discussion

(1) Dilute Regime. The low-concentration range corresponds to dilute solutions, where the polymer chains act as individual units. The dominant parameter is the coil radius of gyration. Since sedimentation is a dynamic technique, the sedimentation coefficient has to be related to the hydrodynamic radius R_H. Therefore

$$s \propto M/R_H \tag{25}$$

From our experimental law at infinite dilution, we deduce that

$$R_H \propto M^{0.50}$$

for flexible chains in Θ solvents. This is a well-known result, which has also been established by quasi-elastic light scattering[6] and viscometry[26] techniques. Our expression $s_0 = (1.50 \pm 0.01) \times 10^{-15} M^{0.50}$ can also be directly compared with numerous earlier determinations using analytical ultracentrifugation.[5,7,27-29] The agreement is excellent for both the prefactor and the exponent of the molecular weight dependence. It is to be noted that our data encompass a larger molecular weight range than generally studied because of our 20.6 × 10^6 sample.

There is a slight concentration dependence of the s values in the dilute regime. It is customary to write

$$\frac{1}{s} = \frac{1}{s_0}(1 + k_s c) \tag{26}$$

Using our sedimentation data obtained at low concentrations for the various molecular weights, we obtain

$$k_s = (0.052 \pm 0.010) M^{1/2} \text{ cm}^3 \text{ g}^{-1}$$

This is in agreement with the expression

$$k_s = (0.062 \pm 0.003) M^{1/2} \text{ cm}^3 \text{ g}^{-1}$$

established with great care by Mulderije[7] for the polystyrene–cyclohexane system at the Θ temperature. This author emphasizes that, contrary to a recent theory by Freed,[30] k_s is not equal to the intrinsic viscosity $[\eta]$ but simply proportional to $[\eta]$ with a prefactor smaller than unity. It is to be noted that the older Pyun–Fixman theory,[31] eventually slightly modified,[32,33] gives a much better description of our experimental data.

(2) Semidilute Regime. At the highest concentrations studied, the chains are interpenetrating and local intermolecular interactions become important. As a consequence the relevant length is no longer the chain radius of gyration R_H but the dynamic correlation distance ξ_H ($\xi_H < R_H$). This explains why the sedimentation coefficient becomes molecular weight independent. We have actually used this criterion to help and select the data points belonging to the semidilute regime.

From the concentration dependence of the sedimentation coefficient, we get

$$\xi_H \propto c^{-0.96 \pm 0.04}$$

in good agreement with the scaling predictions. Comparing this result with the neutron determination of the static correlation length,[8] we find that the two quantities scale with the same exponent.

In a very recent independent measurement, Roots and Nyström have obtained an almost identical result, $\xi_H \propto c^{-0.95 \pm 0.06}$, in the same polystyrene–cyclohexane system.[34] They used a somewhat different experimental method based on the measurement of the cooperative mass diffusion that occurs when contacting two solutions of different solute concentrations.

A controversial point deserves some discussion. In the above, we have always interpreted the c^{-1} concentration dependence of the sedimentation coefficient at high concentrations in the framework of the scaling theory. However, it is formally possible to derive the same result from a simple extrapolation of the empirical formula $s = s_0(1$

Table VI
End-to-End Distance L_H and Radius of Gyration R_H Calculated from the Crossover Concentration c^*

$10^{-6}M_w$	10^3c^*, g cm^{-3}	L_H calcd from c^*, Å	$R_H = L_H/6^{1/2}$ calcd from c^*, Å	$R_H = 0.223M_w^{1/2}$ calcd from ref 35, Å
20.6	1.43 ± 0.07	2882	1180 ± 20[a]	1043
8.42	2.28 ± 0.07	1831	750 ± 20	667
3.84	3.30 ± 0.05	1246	508 ± 3	451
1.26	5.80 ± 0.10	712	291 ± 2	258
0.422	10.5 ± 0.3	406	166 ± 2	150

[a] The uncertainty includes possible errors in the c^* determination but neglects polydispersity.

$+ k_sc)^{-1}$, valid at low concentrations. Indeed, if $k_sc \gg 1$, s can be written as $s = s_0(k_sc^{-1})$ and since both s_0 and k_s vary with molecular weight as $M^{1/2}$, one gets the final result $s \propto c^{-1}$, independent of molecular weight. Using our experimental determination of $s_0 = 1.50 \times 10^{-15}M^{1/2}$ and $k_s = 0.052M^{1/2}$, it is even possible to predict the proportionality coefficient. At high concentration, s should vary as

$$s \simeq 3 \times 10^{-1}c^{-1}$$

Although attractive, this approach is nevertheless incorrect for several reasons: (i) The expression used in the derivation cannot be extended to high concentrations without introducing additional terms. Its theoretical basis, as laid out by Pyun and Fixman,[31] supposes that higher than binary interactions between the sedimenting particles are neglected. (ii) When the chains start to overlap, the polymer segment density becomes homogeneous throughout the solution and sedimentation no longer involves the flow of solvent around coils considered as impenetrable spheres but rather the flow of solvent through interpenetrated chains forming a porous plug with a characteristic mesh size ξ.[11,14-16] (iii) Finally, it should be remarked that the calculated prefactor of 3×10^{-14} disagrees with our own experimental determination of 1.15×10^{-14} (see Figure 4).

(3) Crossover Concentration c^*. The crossover concentration c^* corresponds to the solute concentration for which the individual chains start to overlap. One of its possible definitions is to say that it occurs when the bulk concentration becomes comparable to the average concentration within a single coil.

$$c^* \propto M/R_H^3 \qquad (27)$$

Using our experimental molecular weight dependence of c^*, $c^* \propto M^{-0.50}$, we readily confirm that

$$R_H \propto M^{0.50}$$

for ideal polystyrene chains in cyclohexane. Absolute values for R_H can be obtained defining $c^* = M/\mathcal{N}_AL_H^3$, where L_H is the end-to-end distance ($L_H = 6^{1/2}R_H$). The results are reported in Table VI and compared with the master equation $R_H = 0.223M^{0.50}$ proposed by Akcasu and Han.[35] The correspondence is good although care must be exercised. It is known that the coil dimensions of a given polymer sample are not exactly the same in all Θ solvents due to the effect of the solvent on the short-range, e.g., steric, interactions along the polymer chain.[36]

It is interesting to repeat the same analysis on our previously published data[25] for swollen chains dissolved in good solvents (polystyrene–benzene solutions). This is done in Figure 7 in which we have plotted the dependence of c^*_{GS} as a function of molecular weight. We obtain

$$c^*_{GS} \propto M^{-0.66\pm0.03}$$

and therefore

$$(R_H)_{GS} \propto M^{-0.55\pm0.01}$$

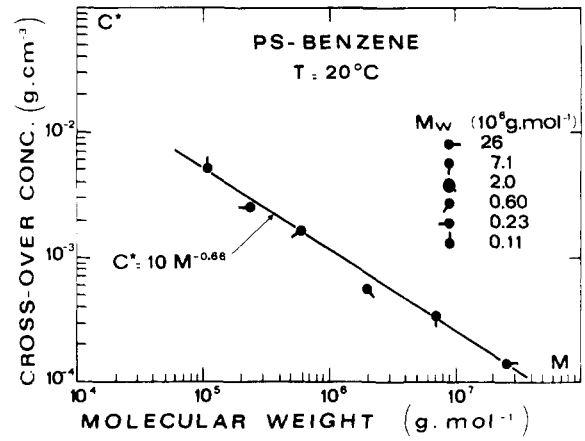

Figure 7. Crossover concentration c^*, as calculated from the data of Figure 2 in ref 23, vs. polymer molecular weight on log–log scales. The slope corresponds to $c^* \propto M^{-0.66}$. Polystyrene–benzene solutions at room temperature.

Contrary to the Θ solvent case, the exponent for the hydrodynamic radius of gyration R_H is markedly lower than its static counterpart R_G since $(R_G)_{GS} \sim M^{0.59}$.[37] This observation permits one to explain why the c^* values obtained by ultracentrifugation in good and Θ solvents, respectively, are not more widely spaced apart. From the above result, it is expected that the ratio c^*_Θ/c^*_{GS} measured in dynamic experiments will be given by

$$c^*_\Theta/c^*_{GS} \sim N^{0.16}$$

where N is the degree of polymerization.[3] The 0.16 exponent value of the molecular weight dependence is much lower than the one found for static experiments. Indeed, in the static case, one obtains

$$c^*_\Theta/c^*_{GS} \sim N^{0.27}$$

For the large-N chains used in the present study, the difference between dynamic and static experiments is therefore particularly noticeable. If $N \simeq 10^4$ (i.e., $M \simeq 10^6$), the ratio is 6.3 in the first case and increases to 22.4 in the second.

There are several determinations of the concentration of first overlap in the literature. Cornet[38] has measured c^* from the onset of straight-line behavior when plotting the zero shear viscosity η_0 vs. concentration on logarithmic scales. He has also verified the Simha relationship[39] between the c^* for spherical, nondraining, impenetrable coils and the intrinsic viscosity $[\eta]$. Experimentally, it was found that $c^* = 0.614/[\eta]$ for the polystyrene–cyclohexane system. Graessley has also suggested[40] a different expression, $c^* = 0.77/[\eta]$, independent in first approximation of the polymer–solvent system for linear chains. However, it is very clear that the proportionality coefficient depends on the exact definition of the overlap concentration and may well vary by a factor of 2. Using the viscosity data of Einaga et al.[41] for polystyrene–cyclohexane at $T = 34.5$

Table VII
Comparison between c^* Values Determined by Sedimentation and the Intrinsic Viscosity Data of Ref 41 for the Various Molecular Weight Fractions in the Same Polymer-Solvent System[a]

$10^{-6}M_w$	10^3c^*, g cm^{-3}	$10^{-2}[\eta]_\Theta$, cm^3 g^{-1}	$c^*[\eta]_\Theta$
20.6	1.43 ± 0.07	3.994	0.57 ± 0.03
8.42	2.28 ± 0.07	2.554	0.58 ± 0.02
3.84	3.30 ± 0.05	1.724	0.57 ± 0.02
1.26	5.80 ± 0.10	0.988	0.58 ± 0.02
4.22	10.5 ± 0.3	0.572	0.60 ± 0.02

[a] It is checked that the product $c^*[\eta]_\Theta$ is a constant = 0.58 ± 0.03.

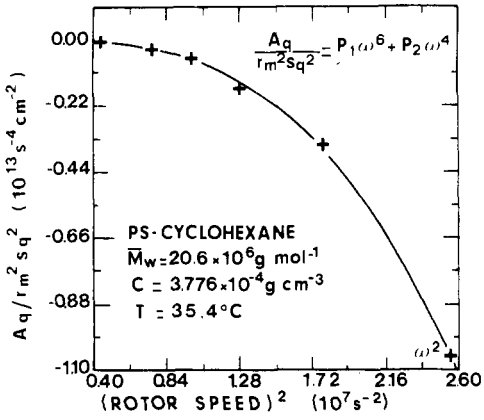

Figure 8. Dependence of the quadratic parameter A_q vs. rotor speed during the sedimentation run for the 20.6 × 10^6 molecular weight fraction. The solid line corresponds to the best fit with the function $P_1\omega^6 + P_2\omega^4$, where P_1 and P_2 are two coefficients. All experiments have been performed at c = 3.77 × 10^{-4} g cm^{-3}.

°C, we have tried to see if a similar relationship holds true in our case. This is done in Table VII. The product $c^*[\eta]$ is indeed a constant, independent of molecular weight. Its value of 0.58 ± 0.03 is very close to the Cornet result.[38]

(4) Pressure and Concentration Dependence of the Sedimentation Coefficient. We can derive the coefficient μ of the pressure dependence of the sedimentation coefficient from our experiments at fixed molecular weight and concentration but at different rotor speeds. Equation 17 gives the relationship between the quadratic coefficient A_q, μ, and k_s. μ is readily derived from the ω^6 term, while k_s is derived from the ω^4 term. In Figure 8, we have plotted the A_q values for six different runs performed at speeds ranging from 20 000 to 48 100 rpm. All samples were taken from the same solution of concentration c = 3.77 × 10^{-4} g cm^{-3} and M = 20.6 × 10^6. The curve is shown as $A_q/r_m^2 s_q^2$ vs. ω^2. The solid line is the theoretical curve $P_1\omega^6 + P_2\omega^4$, where P_1 and P_2 are two adjustable parameters. The best fit to the data points yields $P_1 = -(6.2 \pm 0.1)\ 10^{-10}$ s^{-2} cm^{-2} and $P_2 = -(6 \pm 1) \times 10^{-4}$ cm^{-2}. In the investigated speed range the ω^6 term is dominant and the ω^4 term represents only a 10% correction. This explains why P_1, and therefore μ, is determined with a much better accuracy than P_2 and its associated parameter k_s. From $P_1 = -1/2\rho_0^0\mu$ and taking ρ_0^0 = 0.778 g cm^{-3},[42] we obtain

$$\mu = (1.60 \pm 0.05) \times 10^{-8}\ \text{Pa}^{-1}$$

This value is in excellent agreement with the existing literature data, which are in the range (1.2–2.0) × 10^{-8} Pa^{-1}.[5,23,43] Direct calculations from independent physical data for the cyclohexane–polystyrene system give μ = 2.0 × 10^{-8} Pa^{-1}.[5] The k_s coefficient is derived from $P_2 = -(c_m/r_m^2)[f'(c_m)/f(c_m)]$. For experiments performed in the dilute regime, P_2 can be rewritten as $P_2 = -(c_m k_s/r_m^2)(1 + k_s c_m)^{-1}$. As already stated, the accuracy of P_2 and therefore on k_s is not very good. It is observed that k_s falls in the range 50–150 cm^3 g^{-1} for our 20.6 × 10^6 molecular weight sample. This value is not unreasonable compared with our direct preceding determination using the s concentration dependence in the dilute regime.

VII. Conclusion

The present experiments have been performed on high enough molecular weight materials and over a large enough concentration range to allow for the investigation of the sedimentation behavior of flexible ideal macromolecular chains in the dilute and semidilute concentration ranges of Θ solutions. The sedimentation data have been analyzed in the framework of the scaling theory. Some of the obtained results, e.g., the molecular weight dependence of the hydrodynamic radius of gyration $R_H \sim M^{0.50}$ and that of the crossover concentration $c^* \sim M^{-0.50}$, were already well-known from similar ultracentrifugation experiments in the first case or from viscosity data in the second. The concentration dependence of the hydrodynamic correlation length $\xi_H \sim c^{-0.96}$ is more novel. The associated characteristic exponent is close to the corresponding static exponent measured by neutron experiments for ideal chains. Moreover, it agrees with a recent independent dynamic determination using a gradient diffusion technique. We have also provided good evidence that the crossover concentration between the dilute and the semidilute regimes is particularly clear-cut in Θ solutions. Our determination is in very close quantitative agreement with independent viscometric data since it is found that $c^* = 0.58/[\eta]$ in one case and $c^* = 0.61/[\eta]$ in the other.

The present experiments demonstrate that the ultracentrifugation technique can provide a very complete picture of the hydrodynamic properties of Θ polymer solutions. It has the advantage over dynamic light scattering of being quite insensitive to the presence of dust particles and of being applicable up to the highest molecular weight chains without the danger of probing internal modes. It has also the advantage over viscoelastic measurements of being performed automatically to zero shear, with no need for extrapolation. It is clear, however, that some precautions are necessary. Due to two additional effects, i.e., the dilution due to the cell sector shape and the hydrostatic pressure generated by the liquid column between the meniscus and the solvent–solution boundary, the displacement of the sedimentation peak obeys a quadratic rather than a linear function of time. Neglecting this correction would lead to results in error by as much as 20%. On the other hand, taking these effects into account yields both the coefficient μ of the pressure dependence of the sedimentation coefficient and also the coefficient k_s of its concentration dependence.

After this work was completed, we learned that similar experiments have been performed by Roots and Nyström on the polystyrene–cyclopentane system.[44] Their values of the characteristic exponents for the crossover concentration and the dynamic correlation length fully corroborate our own results. Our data are, however, more extensive since they cover a larger range of molecular weights and of concentration in the semidilute regime (typically 4 molecular weights above 10^6 instead of 2 and 2 decades in concentration instead of 1).

References and Notes

(1) Flory, P. J. "Principles of Polymer Chemistry"; Cornell University Press: Ithaca, NY, 1953.
(2) Stephen, M. *Phys. Lett.* **1975**, *53A*, 363.
(3) de Gennes, P.-G. "Scaling Concepts in Polymer Physics"; Cornell University Press: Ithaca, NY, 1979.

(4) Daoud, M.; Jannink, G. *J. Phys. (Paris)* **1976**, *37*, 973.
(5) Kotaka, T.; Donkai, N. *J. Polym. Sci.* **1968**, *6*, 1457.
(6) See, for example: Nose, T.; Chu, B. *Macromolecules* **1979**, *12*, 1122. Jones, G.; Caroline, D. *Chem. Phys. Lett.* **1979**, *37*, 187.
(7) Mulderije, J. J. H. *Macromolecules* **1980**, *13*, 1207.
(8) Cotton, J. P.; Nierlich, M.; Boué, F.; Daoud, M.; Farnoux, B.; Jannink, G.; Duplessix, R.; Picot, C. *J. Chem. Phys.* **1976**, *65*, 1101.
(9) Roots, J.; Nyström, B. *Polymer* **1979**, *20*, 149, 157.
(10) Adam, M.; Delsanti, M. *J. Phys. (Paris)* **1980**, *41*, 713.
(11) de Gennes, P.-G. *Macromolecules* **1976**, *9*, 587.
(12) Vidakovic, P.; Allain, C.; Rondelez, F. *J. Phys. (Paris)* **1981**, *42*, 323.
(13) Schachman, H. K. "Ultracentrifugation in Biochemistry"; Academic Press: New York, 1959.
(14) Brochard, F.; de Gennes, P.-G. *Macromolecules* **1977**, *10*, 1157.
(15) Weill, G.; des Cloizeaux, J. *J. Phys. (Paris)* **1979**, *40*, 99.
(16) Minjlieff, P.; Jaspers, W. *Trans. Faraday Soc.* **1971**, *67*, 1837.
(17) Slagowski, E.; Tsai, B.; McIntyre, D. *Macromolecules* **1976**, *9*, 687.
(18) Swislow, G.; Sun, S. T.; Nishio, I.; Tanaka, T. *Phys. Rev. Lett.* **1980**, *44*, 796.
(19) Fujita, H. "Foundations of Ultra-Centrifugal Analysis"; Wiley: New York, 1975.
(20) Dishon, M.; Weiss, G. H.; Yphantis, D. A. *J. Polym. Sci.* **1970**, *8*, 2163.
(21) Yamakawa, H. "Modern Theory of Polymer Solutions"; Harper and Row: New York, 1971.
(22) Nyström, B.; Porsch, B.; Sundelöf, L. O. *Eur. Polym. J.* **1977**, *11*, 683.
(23) Destor, C.; Rondelez, F. *Polymer* **1981**, *22*, 67.
(24) Tournarie, G. *J. Phys. (Paris)* **1969**, *30*, 737.
(25) Destor, C.; Rondelez, F. *J. Polym. Sci., Polym. Lett. Ed.* **1979**, *17*, 527.
(26) Inagaki, H.; Suzuki, H.; Kurata, M. *J. Polym. Sci., Part C* **1966**, *15*, 409.
(27) Cantow, H. J. *Makromol. Chem.* **1959**, *30*, 169.
(28) Kotera, A.; Hamada, T. *Rep. Prog. Polym. Phys. Jpn.* **1968**, *11*, 61.
(29) Cowie, J. M. G.; Cussler, E. L. *J. Chem. Phys.* **1967**, *46*, 4886.
(30) Freed, K. F. *J. Chem. Phys.* **1976**, *52*, 4212.
(31) Pyun, C. W.; Fixman, M. *J. Chem. Phys.* **1964**, *41*, 937.
(32) Mulderije, J. J. H. *Macromolecules* **1980**, *13*, 1526.
(33) Vrentas, J. S.; Liu, H. T.; Duda, J. L. *J. Polym. Sci., Polym. Phys. Ed.* **1980**, *18*, 1633.
(34) Roots, J.; Nyström, B. *Macromolecules* **1980**, *13*, 1595.
(35) Akcasu, A. Z.; Han, C. C. *Macromolecules* **1979**, *12*, 276.
(36) Munk, P.; Gutierrez, B. O. *Macromolecules* **1979**, *12*, 467.
(37) Miyaki, Y.; Einaga, Y.; Fujita, H. *Macromolecules* **1978**, *11*, 1180.
(38) Cornet, C. F. *Polymer* **1965**, *6*, 373.
(39) Weissberg, S. G.; Simha, R.; Rothamn, S. *J. Res. Natl. Bur. Stand.* **1951**, *47*, 298. Simha, R.; Utracki, L. *Rheol. Acta* **1973**, *12*, 455.
(40) Graessley, W. W. *Polymer* **1980**, *21*, 258.
(41) Einaga, Y.; Miyaki, Y.; Fujita, H. *J. Polym. Sci., Polym. Phys. Ed.* **1979**, *17*, 2103.
(42) Brandrup, J.; Immergut, E. H., Eds. "Polymer Handbook"; Wiley: New York, 1975.
(43) Billick, I. H. *J. Phys. Chem.* **1962**, *66*, 1941.
(44) Roots, J.; Nyström, B. *J. Polym. Sci., Polym. Phys. Ed.* **1981**, *19*, 479.

High-Performance Liquid Chromatography of Poly(tetramethylene ether) Glycols

G. D. Andrews,[1] A. Vatvars,[1] and G. Pruckmayr*[2]

Central Research and Development Department and Chemicals and Pigments Department, E. I. du Pont de Nemours and Company, Inc., Experimental Station, Wilmington, Delaware 19898. *Received March 30, 1982*

ABSTRACT: A high-performance liquid chromatographic method for the analysis of poly(tetramethylene ether) glycols has been developed. In contrast to gel permeation chromatography, the new technique allows efficient separation of these polyethers into individual oligomers and thus affords more information about the polymer. Liquid chromatograms are compared with gel permeation chromatograms, and the advantages and limitations of the new technique are discussed.

Introduction

The most important criteria that physically characterize a linear polymer are molecular weight and molecular weight distribution. Number-average molecular weight M_n of poly(tetramethylene ether) glycol (PTMEG) is most accurately determined by titration (acetic anhydride or phthalic anhydride method)[3] or by spectroscopic methods (calibrated IR scans, end-group determination by NMR, etc.).[4] Weight-average molecular weight M_w and polydispersity M_w/M_n are less easily determined, and the latter is frequently approximated by an empirical viscosity ratio M_{wv}/M_n, determined from polymer bulk viscosity at a specified temperature.[5]

The weight-average molecular weight M_w is usually measured by gel permeation chromatography (GPC), which partially fractionates the polymer sample by retaining the shorter chains longer in the porous column packing and allowing the longer chains to pass through the column faster. The resulting chromatogram is a plot of polymer concentration in the eluant vs. elution time, with the highest molecular weight fractions recorded first. After calibration with samples of known molecular weights, GPC elution time can be converted to molecular weight and is generally plotted on a log scale. Figure 1 shows typical GPC scans of commercial poly(tetramethylene ether) glycols of number-average molecular weights 1000 and 2000. The weight-average molecular weights of these samples, calculated from the GPC data, were 1720 and 3420, respectively.

The newer, high-efficiency μ-Styragel column packings improve fractionation to a point where the individual oligomer fractions are partially separated, particulalrly when several columns are used in series (Figure 2). Complete separation of some fractions on a vinyl acetate gel has been described[6] and separation of all fractions can, in principle, be achieved by GPC using extremely long columns and consequently long elution times.[7] However, we were looking for a more efficient method of separating PTMEG into its individual oligomers, on both an analytical and a preparative scale.

Adsorption chromatography on silica gel columns had been tried earlier, and although some molecular weight

0024-9297/82/2215-1580$01.25/0 © 1982 American Chemical Society